NATURAL FIBRE TEXTILE CHARACTERIZATION FOR DUAL-SCALE FLOW PREDICTION

Yannick Blößl[1], Ralf Schledjewski[2]

[1]Processing of Composites Group, Department Polymer Engineering, Montanuniverstität Leoben, Otto Glöckel-Straße 2, A-8700 Leoben, Austria
Email: yannick.bloessl@unileoben.ac.at, Web Page: http://www.kunststofftechnik.at
[2]Processing of Composites Group, Department Polymer Engineering, Montanuniverstität Leoben, Otto Glöckel-Straße 2, A-8700 Leoben, Austria
Email: ralf.schledjewski@unileoben.ac.at, Web Page: http://www.kunststofftechnik.at

Keywords: Liquid Composite Moulding, Capillary Rise, Natural Fibre, Textile Characterization

Abstract
Motivated by the minimisation of the void content inside a composite part and the optimisation of the impregnation step in Liquid Composite Moulding processes, this study focuses on the characterization of natural fibre textiles with regard to the capillary action inside this porous media. Fluid flow mechanisms acting on macro- and micro level inside the fibrous structure and have to be considered to prevent the formation of voids inside the composite. The goal of this work is the evaluation of the effective size of capillaries in a natural fibre textile. Capillary rise experiments were carried out on a flax fibre fabric with two different test fluids (n-Decan and 2-Propanol). The model used for the evaluation based on the Lucas-Washburn equation. This approach led to consistent results for the effective capillary radius in the initial stage of the experiment and independent of the test fluid. Divergences between the underlying model and the experiment results were present with advancing capillary rise. Based in the test results unconsidered effects are pointed out that provide an explanation for the observed wicking behaviour.

1. Introduction

Liquid Composite Moulding (LCM) processes have developed over the past years to become one of the main techniques for the production of high-quality fibre-reinforced composites. Reinforcing materials consist mainly of synthetic fibres like glass, carbon and aramid. Regarding to ecological factors some natural fibres represent a sustainable alternative for the reinforcing component of a composite structure. Cellulose based plant fibres like flax and hemp provide high stiffness and moderate strength which can be used as renewable resource for lightweight components.
A critical step of the LCM process chain is the infiltration of the porous reinforcing structure with a liquid resin system, as insufficient saturated regions and voids could drastically reduce the mechanical properties of the final part. In many cases the porosities inside a dry reinforcing textile have a multi-scale character. While micro-porosities inside yarns or rovings are present on intra-tow level, macro-porosities are present between the fibre bundles on inter-tow level. Depending on the resulting permeabilities on micro- and macro-scale two phenomena are governing the impregnation process: The fluid flow driven by viscous forces (dominant on inter-tow level) and capillary effects (dominant on intra-tow level) [1]. This leads to a situation where unsuitable process conditions during impregnation can cause voids in the final composite part. The mechanisms of void formation in connection with the current issue are depicted in figure 1. A critical state is present when the viscous or the capillary fluid flow dominates and leads to a flow front shape prone to air entrapment and void formation inside the fibre bundle (intra-tow porosity) or between them (inter-tow porosity).

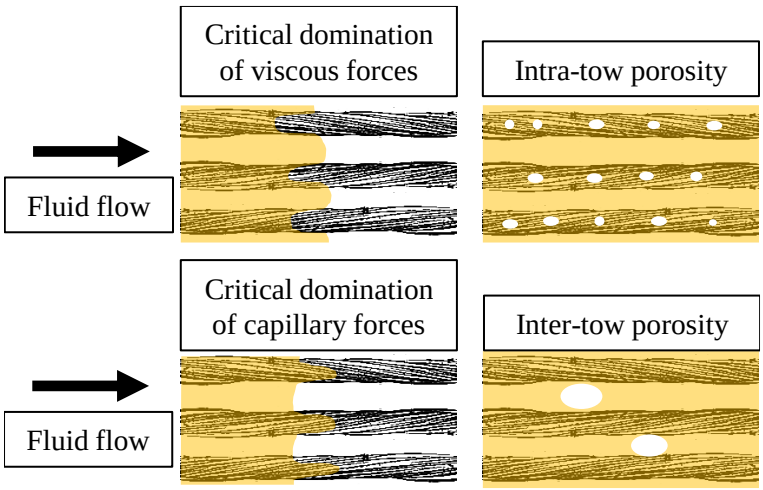

Figure 1. Mechanisms of void formation during impregnation

In fluid dynamics, the dimensionless capillary number *Ca* is used to describe the importance of the viscous force relative to the capillary force for the present fluid flow [2]. The capillary number is defined as follows in (Eq. 1):

$$Ca = \eta \cdot v / \gamma_{ls} \tag{1}$$

and relates the dynamic viscosity of the fluid η with the characteristic velocity of the fluid flow *v* and the surface tension between the liquid and the solid phase γ_{ls}. Based on these mechanisms the velocity of the fluid and the state of viscous and capillary forces during impregnation directly influence the quality of the final composite. This effect was demonstrated by several authors who deduced a correlation between the capillary number and the resulting void content inside the composite material after impregnation [3–7]. By changing the impregnation speed, optimum flow velocities were determined which led to a minimal amount of intra-tow and inter-tow porosities. The right balance between viscous and capillary driven flow velocities seems therefore to be an important factor for an optimisation of the infiltration process. While the viscous flow is basically controlled by the external applied pressure, the capillary flow takes place on a microscopic level in the textile and depends on the properties of the fluid and fibre-surface and the fibrous architecture. It is therefore necessary to get deeper understanding of the capillary action inside the textile structures.

This work focuses on the evaluation of the present capillary radii in a flax fibre textile using capillary rise experiments. With this geometric textile specific parameter, it is possible to use further approaches according the wicking properties of the reinforcement dependent on the fluid properties and can be used to define optimal process conditions for the textile impregnation.

The experiments in this work based on the Lucas-Washburn model (Eq. 2), which describes the dynamics of liquid flow in a capillary tube [8]:

$$h^2 = (r_c \cdot \gamma_l \cdot \cos(\theta) / (2 \cdot \eta)) \cdot t = m \cdot t \tag{2}$$

where *h* is the height of the capillary rise over time *t*, γ_l and η are the fluid surface tension and the dynamic viscosity respectively, θ is the contact angle between the liquid and the solid phase and r_c is the capillary radius. With constant values for r_c, θ, γ_l and η this model leads to a linear relationship between the squared fluid height h^2 over time *t*, which is defined by the slope

$m = r_c \cdot \gamma_l \cdot cos(\theta) / (2 \cdot \eta)$. By way of illustration, figure 2 shows on the left side a schematic representation of the capillary action and the geometric parameter in the Lucas-Washburn Equation (Eq. 2).

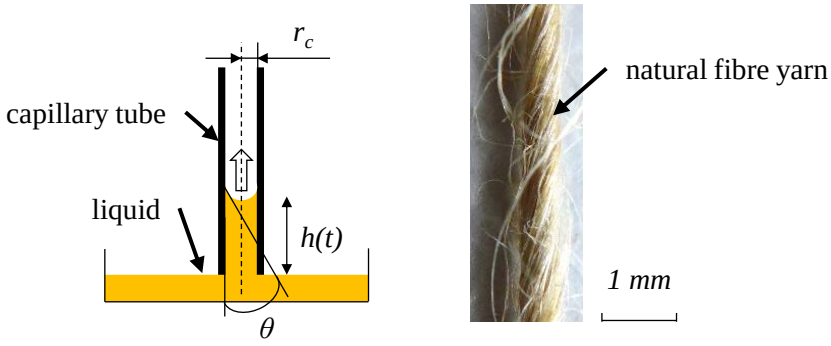

Figure 2. Schematic of the capillary rise in a tube (left). Structure of a natural fibre yarn (right)

Although this model simplifies the situation of capillary rise in a textile structure with the assumption of cylindrical capillaries with constant radius and the neglect of gravitational, inertia and viscous forces, it was used, at least as basic approach for further modifications, in several studies [9–13]. The capillary flow along parallel fibres in a bundle is then approximated as a bundle of parallel capillary tubes. Figure 2 shows on the right side the structure of a typical natural fibre yarn. The more irregular fibre architecture due to variations in fibre diameter, the drill of the yarn, non-endless fibre lengths and protruding fibres lead to an even higher divergence between the underlying model and the real situation. Therefore, the consistency of the Lucas-Washburn model will be proven and differences between the prospective behaviour and the experimental results will be discussed.

2. Experimental setup and test procedure

Figure 3 shows a picture of the test rig used for the capillary rise experiments in this work. The setup consists of the sample holder with the textile to be characterized and a test fluid container beneath it. A lifting platform is used for the positioning of the fluid container. An industrial camera records sequentially the textile saturation in the sample holder. The sample holder consists of two transparent glass blocks clamped in between two U-shaped metal parts. The textile sample is placed between the two glass blocks with the edge of the textile in alignment with the open edge at the bottom of the sample holder. With distance frames between the glass blocks the height of the textile sample can be adjusted. With the start of the experiment the stage lifts up and brings the test fluid in contact with the open edge of the textile sample in the sample holder. The fluid then flows up inside the porous textile by capillary action. The industrial camera captures pictures of the textile sequentially during the experiment time. Afterwards the camera images are used to detect to height of capillary rise over time by using digital image processing techniques.

The textile used for the experiments is a non-crimp unidirectional flax fabric provided by Bcomp® (ampliTex® 5009). The areal weight and the fibre density ρ_f are 0.300 kg/m² and 1580 kg/m³, respectively. The fibre density was measured with a He-pycnometer (Ultrapycometer 1000, Quantachrome Instruments) and a precision scale (LabStyle 204, Mettler Toledo). The size of the textile samples is 60 mm by 65 mm in width w and length l, respectively. To avoid any influences from the upper edge of the textile sample at a height of 65 mm the range for the evaluation was set to a maximum height of 60 mm. Test samples with eight and ten layers were prepared, while the cavity height d was set constant for all measurements to 4 mm. With the mass of the textile sample the fibre volume fraction V_f was calculated with the following equation (Eq. 3):

$$V_f = m / (w \cdot l \cdot d \cdot \rho_f) \quad (3)$$

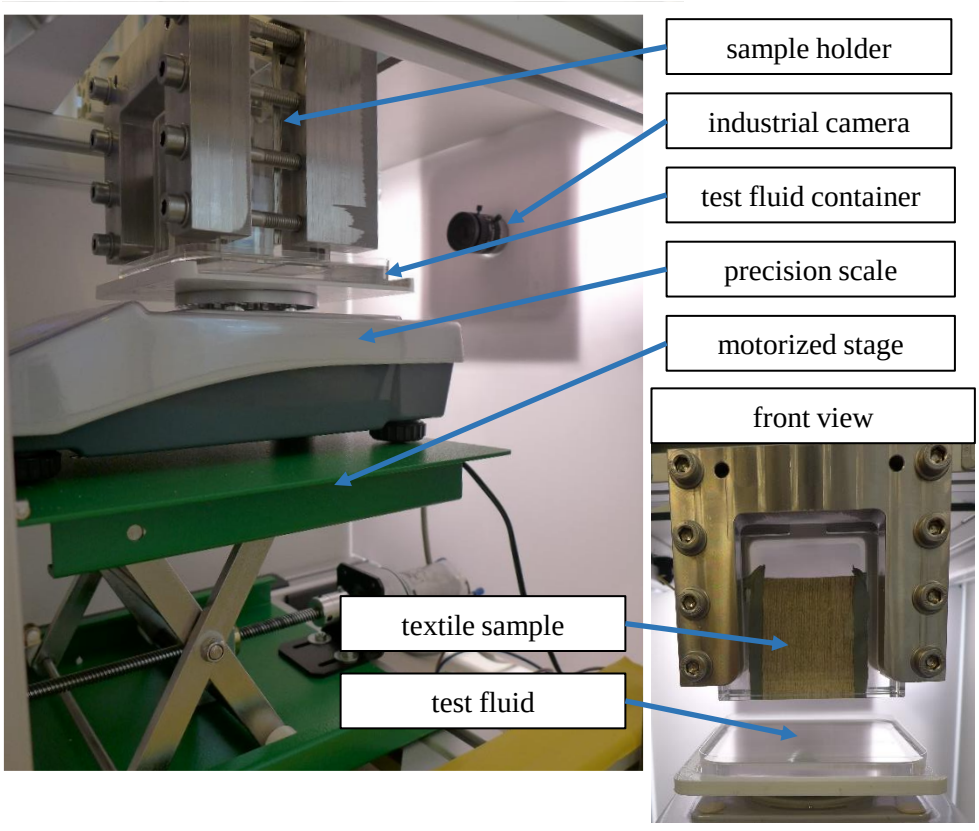

Figure 3. Test rig for capillary rise experiments

Test fluids were n-Decan and 2-Propanol. Table 1 presents the relevant fluid properties at 25 °C, as found in literature [14]. n-Decan was selected for its low totally dispersive surface tension. 2-Propanol in comparison shows a slightly lower surface tension than n-Decan, a higher viscosity and density. The two selected fluids show different dynamics during the capillary rise experiments. The usage of two different fluids was used to verify the resulting textile specific capillary radii, which should not be effected by the fluid properties.

Table 1. Test fluid properties at 25 °C [14]

	surface tension γ_l ($\cdot 10^{-3}$ N m^{-1})	*viscosity* η ($\cdot 10^{-3}$ Pas)	*density* ρ (kg m^{-1})
n-Decan (DEC)	23.37	0.838	725.5
2-Propanol (IPA)	20.93	2.038	780.9

With the significantly lower surface tension of both fluids compared to the free surface energy of flax fibre, which is in the range of $62 \cdot 10^{-3}$ N m^{-1} [15], a full wetting behaviour with a contact angle θ of 0° between fluid and fibre surface was assumed for the test evaluation.

3. Results

The diagram in figure 4 shows the evolution of the squared flow front over time for two experiments using n-Decan and 2-Propanol as test fluids. The textile samples were prepared with ten layers respectively, which lead to a similar fibre volume fraction in both experiments. As can be seen, the capillary rise of n-Decan is faster compared to 2-Propanol. The final height of 60 mm was reached with n-Decan and 2-Propanol after 24.8 sec and 89.6 sec, respectively. This result is consistent with the higher penetrativity of n-Decan due to its lower viscosity compared to 2-Propanol.
Furthermore, it can be seen that both curves in the h^2-t-diagram do not follow a linear trend over the whole experiment time like it is proposed by the Lucas-Washburn Model in (Eq. 2), when constant values respectively for the capillary radius r_c, the fluid properties (γ_l, η) and the contact angle θ are assumed. Both curves show rather a faster progression of the squared height at the start of the experiment and a shift to lower progression rates at higher capillary heights.

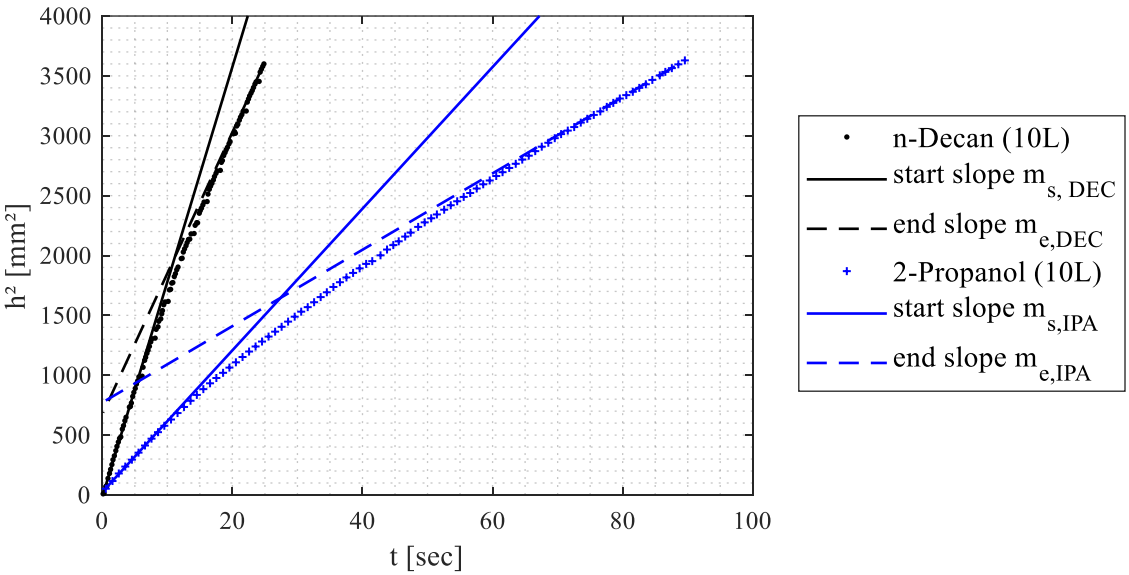

Figure 4. Squared capillary rise over time with straight line fits for two experiments with 10-layer textile samples tested with n-Decan and 2-Propanol

The deviation from the linear curve progression based on the Lucas-Washburn model (Eq. 2) can be explained by a decrease of the effective capillary radius with an advancing flow front. For the calculation of the effective capillary radii the slopes of the h^2-t-curves at the start and the end of the experiment were defined using linear curve fitting based on the least square fit method. The number of data points, which are used for the straight line fits, was defined by the maximal coefficient of determination R^2 value that could be reached with the fit from both ends of the h^2-t-curve, but not less than three points. In the present case this approach led to a reliable strategy for the determination of the slope values m. In figure 4 the resulting straight lines are shown for the plotted experiment data. The associated values for the slopes are as follows: $m_{s,DEC} = 183.3$ mm²/s ($R^2 = 0.9979$), $m_{e,DEC} = 129.5$ mm²/s ($R^2 = 0.9986$), $m_{s,IPA} = 59.1$ mm²/s ($R^2 = 0.9996$) and $m_{e,IPA} = 31.9$ mm²/s ($R^2 = 0.9999$). With the assumption that a contact angle of zero is present for both fluids, the effective capillary radius $r_{c,eff}$ was calculated with the following equation (Eq. 3):

$$r_{c,eff} = (2 \cdot \eta \cdot m) / \gamma_l \tag{3}$$

The resulting values for $r_{c,eff}$ over the fibre volume fraction for all performed experiments are shown in the diagrams of figure 5. On the left side the effective capillary radii based on the start slopes are depicted. The diagram on the right side contains the related values based on the end slopes. For both test fluids a reduction of $r_{c,eff}$ with higher fibre volume fraction can be observed. A comparison of the values in both diagrams shows also a reduction of the calculated capillary radius from experiment start to end for all tested configurations. The mean $r_{c,eff}$ values for all the tested configurations are $r_{s,DEC,8L}$ = *23.8 µm*, $r_{s,IPA,8L}$ = *26.4 µm*, $r_{s,DEC,10L}$ = *13.1 µm* and $r_{s,IPA,10L}$ = *13.5 µm* at the experiment start and $r_{e,DEC,8L}$ = *15.3 µm*, $r_{e,IPA,8L}$ = *11.5 µm*, $r_{e,DEC,10L}$ = *8.4 µm* and $r_{e,IPA,10L}$ = *7.2 µm* at the experiment end. The corresponding mean reduction of the effective capillary radius over experiment time for the eight-layer textile samples are *35.7%* and *56.4%*, while the experiments with higher fibre volume fractions lead to a mean reduction of *36.0%* and *46.7%* for n-Decan and 2-Propanol, respectively.

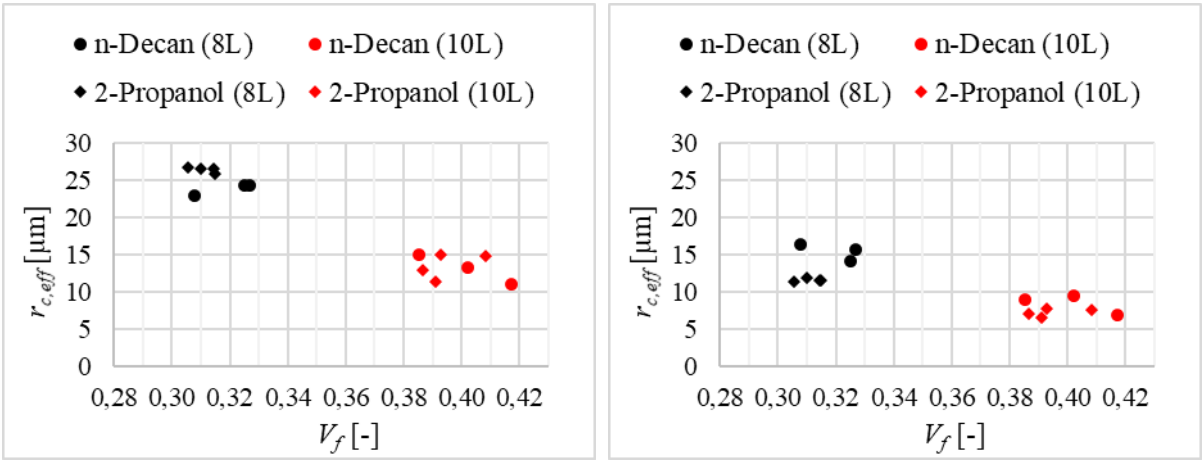

Figure 5. Calculated effective capillary radius over the fibre volume fraction based on the slopes at the start (left) and the end of the capillary rise experiment (right)

4. Discussion

For both fluids the effective capillary radii calculated from the initial start slope of the h^2-t-curves show the same trend with varying fibre volume fraction. And for both fluids the absolute $r_{c,eff}$ values are in the same range for both fluids at low and high fibre volume fractions, respectively. This indicates that the measured value represents a parameter which is defined just by the textile and does not depend on the test fluid properties. This textile-specific parameter can then be used to predict the wicking behaviour with other fluids like liquid resin systems for further process optimisation.
The observed decrease of the effective capillary radii over the experiment time can possibly be traced back to one or more of the following effects which was not considered in the present study.

Fibre swelling:
Unconsidered in the present work was a potential change of the fibre geometry after getting in contact with the test fluids. This effect can occur on natural fibres due to sorption processes and depends on the fibre and fluid properties. Especially high polar liquids like water lead to a noticeable swelling of natural fibres after wetting. This increase of the fibre diameter directly affects the pore size and the capillary rise. Studies on the capillary wicking of natural fibres took the fibre swelling effect into account for describing the observed capillary fluid flow [10,12].

Microscopic tests similar to the method described in [16] but without any drying of the fibres showed no significant change of the flax fibre diameter after wetting with the test fluids used in this study. But as even small changes of the fibre geometry will affect the morphology of the porous architecture this effect should not excluded completely. With the assumption that the partly polar properties of the 2-propanol liquid tend more to effect the fibre size in term of fibre swelling than n-Decan, this effect could explain the higher reduction of the effective capillary radii from the start to the end of the experiment.

Dual scale character of the textile sample:
Wicking tests on glass fibre woven fabrics in [13] show a similar decreasing trend of the square height evolutions over time. The observed progression was related to the dual-scale character of the textile. The macroscopic pores between the fibre bundles lead to a faster fluid progression than in the smaller interstices inside the yarn.

Morphology of capillaries:
In divergence from the underlying assumption of cylindrical capillary tubes with constant radius the capillaries inside the textile structure are an interconnected network of interstices with varying cross section areas. Considering that local pore size reductions will limit the volume flow rate, this effect would lead to a decreasing fluid progression with increasing height, like it was observed in the own experiments.

Gravitational force:
Due to usually much higher maximal liquid heights in capillaries compared to the evaluation range in rise experiments, gravitational forces can be neglected in many cases. But especially for bigger radii and equivalent low capillary pressures or a poor wetting behaviour gravitation could have a significant effect to the capillary rise. For further data, evaluation the influence of gravitational effects should therefore be investigated and possibly be taken into account.

5. Conclusion

In this work the capillary interstices in a natural fibre flax fabric were characterized using capillary rise experiments. Based on the experiment results the Lucas-Washburn equation was used to determine the effective capillary radius inside the fabric. With the use of two test fluids with different wicking dynamics the independence of the fluid properties on the resulting values was proven. It was shown that the calculated values based on the initial situation in the experiment are consistent for both test fluids, which indicates that the resulting geometric value represents a textile specific parameter. With increasing times and advancing flow front a deviation from the Lucas-Washburn model and a slightly higher dependency on the test fluid regarding the resulting capillary radii is present. The observed wicking behaviour was explained by a reduction of the effective capillary radii with advancing capillary rise. Possible effects, not taken into account in the underlying model, were pointed out to examine more accurate modelling approaches in further studies.

Acknowledgments

The work presented in this paper has been elaborated within the context of the project “RSBC - Reliable and Sustainable composite production for Biobased Components". The authors kindly acknowledge the financial support provided by the Austrian Ministry for Transport, Innovation and Technology (bmvit) and the project support from the Austrian Research Promotion Agency (FFG).

References

[1] V. Michaud. A Review of Non-saturated Resin Flow in Liquid Composite Moulding processes. *Transport in Porous Media*, 115:581–601, 2016.
[2] R. W. Johnson, *Handbook of Fluid Dynamics, Second Edition*, CRC Press, s.l., 2016.
[3] F. LeBel, A. E. Fanaei, É. Ruiz and F. Trochu. Prediction of optimal flow front velocity to minimize void formation in dual scale fibrous reinforcements. *International Journal of Material Forming*, 7:93–116, 2014.
[4] N. Patel and L. J. Lee. Modeling of void formation and removal in liquid composite molding. Part II: Model development and implementation. *Polymer Composites*, 17:104–114, 1996.
[5] E. Ruiz, V. Achim, S. Soukane, F. Trochu and J. Breard. Optimization of injection flow rate to minimize micro/macro-voids formation in resin transfer molded composites. *Composites Science and Technology*, 66:475–486, 2006.
[6] J. S. Leclerc and E. Ruiz. Porosity reduction using optimized flow velocity in Resin Transfer Molding. *Composites Part A: Applied Science and Manufacturing*, 39:1859–1868, 2008.
[7] C. H. Park and I. L. Lee. Modeling void formation and unsaturated flow in liquid composite molding processes: A survey and review. *Journal of Reinforced plastics and composites*, 30:957–977, 2011.
[8] E. W. Washburn. The Dynamics of Capillary Flow. *Physical Review*, 17:273–283, 1921.
[9] M. F. Pucci, P.-J. Liotier and S. Drapier. Capillary wicking in a fibrous reinforcement – Orthotropic issues to determine the capillary pressure components. *Composites Part A: Applied Science and Manufacturing*, 77:133–141, 2015.
[10] M. F. Pucci, P.-J. Liotier and S. Drapier. Capillary wicking in flax fabrics – Effects of swelling in water. *Colloids and Surfaces A: Physicochemical and Engineering Aspects*, 498:176–184, 2016.
[11] M. Parada, P. Vontobel, R. M. Rossi, D. Derome and J. Carmeliet. Dynamic Wicking Process in Textiles. *Transport in Porous Media*, 119:611–632, 2017.
[12] G. A. Testoni, S. Kim, A. Pisupati and C. H. Park. Modeling of the capillary wicking of flax fibers by considering the effects of fiber swelling and liquid absorption. *Journal of Colloid and Interface Science*, 525:166–176, 2018.
[13] F. LeBel, A. E. Fanaei, E. Ruiz and F. Trochu. Experimental characterization by fluorescence of capillary flows in dual-scale engineering fabrics. *Textile Research Journal*, 83:1634–1659, 2013.
[14] D. R. Lide, ed., *CRC handbook of chemistry and physics*: *A ready-reference book of chemical and physical data*, CRC Press, Boca Raton, 2003.
[15] C. Baley, F. Busnel, Y. Grohens and O. Sire. Influence of chemical treatments on surface properties and adhesion of flax fibre–polyester resin. *Composites Part A: Applied Science and Manufacturing*, 37:1626–1637, 2006.
[16] H. van Nguyen, M. Lagardère, C. H. Park and S. Panier. Permeability of natural fiber reinforcement for liquid composite molding processes. *Journal of Materials Science*, 49:6449–6458, 2014.